Guided modes in chiroplasma circular waveguides with DB boundaries

A. GHAFFAR[a,b*], Majeed A. S. ALKANHAL[a]
[a]*Dept. of Electrical Engineering, King Saud University, Riyadh, Saudi Arabia*
[b]*Dept. of Physics, University of Agriculture, Faisalabad, Pakistan*

Analytical and numerical analysis of electromagnetic wave propagation in circular waveguides filled with anisotropic chiroplasma media is presented. Emphasis is given to the characteristics of flux density patterns in the waveguide. In the structure of the waveguide, the inner region is assumed to be bounded by Debye boundaries. The characteristics equation for the modes in this waveguide is obtained. The behavior of the dispersion curves and the energy flux are examined numerically. The negative energy flux propagation through the chiroplasma material is confirmed, which clues to exploring the occurrence of negative refraction in chiroplasma medium.

(Received July 3, 2015; accepted September 9, 2015)

Keywords: Wave propagation, Plasma layer, Plasma frequency, Backward waves and energy flux

1. Introduction

The knowledge of wave propagation is important in the present dome of advanced technologies in metamaterial waveguides. The materials waveguides with negative index metamaterials have been investigated by many researchers in microwave to terahertz regime and optical-wave engineering. It is observed that chiral metamaterials are of countless research interest[1, 2]. The chiral media have special characteristics for electromagnetic wave interaction which does not found in natural occurring materials. This media can be used to artificially design device with negative or positive of permittivity and permeability. Several authors carried out researches relevant to isotropic chiral media [3-5].

In order to attain control on chirality in structures like waveguides, certain forms of anisotropy may be produced. It is observed from literatures[6, 7] that uniaxial anisotropic chiral media can yield the phenomenon of backward refraction and easily to be realized. Studies relevant to uniaxial anisotropic chiral metamaterials waveguides have been performed by many researchers [8-10]. Another possibility of fabrication of anisotropic chiral media is by embedding chiral objects in magnetically biased plasma. This chiral embedded magnetically biased plasma materials [11]are referred to as chiroplasma[12, 13].The modal eigenvalue properties in the chiral-plasma medium are, essentially, doubly anisotropic.

This paper deals with a circular waveguide of chiroplasma bounded by DB-boundaries. It was noted in [14]that a parallel-plane waveguide with DB-boundary conditions supports modes that consist of plane waves reflected from both parallel plates. Splitting the modes in TE and TM modes with respect to the normal to both planes, the TE modes turn out to be corresponding to two PEC planes while the TM modes correspond to two PMC planes [15]. The same property has been shown to be valid for the circular waveguide and the spherical resonator with DB-boundaries for TE and TM modes. This is noticed for flux through guides with microstructure twisted clad DB medium and for waves in coaxial optical fiber under DB-boundaries with respect to the radial direction [16-19]. This property was also seen valid in the propagation through uniaxial anisotropic chiral circular waveguide under DB boundaries. Having chirality in the medium, the transformation to circularly or elliptically polarized field from either TE or T M field was attained, which is not the case for an anisotropic filling material.

In this work, we present analysis and computations of the propagation of electromagnetic fields and energy flux density in the chiroplasma-filled cylindrical waveguide employing the DB boundary conditions. The dispersion relations for the guide are derived and used to obtain the propagating modes and their energy flux. Results reveal that the chirality, plasma frequency, and cyclotron frequency of plasma have factual effects on the power values of the propagating modes. The time-harmonic $(j\omega t)$ dependence is adopted and suppressed in what follows.

2. Formulations

Consider a circular waveguide of radius b having an infinite extent along the z-direction which is the optical axis of the circular waveguide. The circular waveguide is filled with a chiroplasma material with its outer surface is defined by the DB boundary. Unit vectors for the cylindrical coordinate system are denoted by $\hat{\rho},\hat{\varphi}$, and $\hat{z}$. The constitutive relations for the chiroplasma medium in the core region are given as

$$\mathbf{D} = \varepsilon_0 \bar{\bar{\varepsilon}} \mathbf{E} + j\gamma \mathbf{H} \tag{1}$$

$$\mathbf{H} = j\gamma \mathbf{E} + \frac{1}{\mu} \mathbf{B} \tag{2}$$

where is the chirality parameter that causes of electromagnetic coupling in the chiroplasma material, is the permeability, and is the permittivity tensor that can be described as

$$\bar{\bar{\varepsilon}} = \begin{vmatrix} \varepsilon_1 & -\varepsilon_2 & 0 \\ \varepsilon_2 & \varepsilon_1 & 0 \\ 0 & 0 & \varepsilon_3 \end{vmatrix} \tag{3}$$

The elements of this tensor are the function of the plasma parameters and their explicit expressions are given as

$$\varepsilon_1 = \varepsilon_0 \left(1 - \frac{\omega_p^2}{\omega^2 - \omega_p^2}\right), \varepsilon_2 = \varepsilon_0 \left(1 - \frac{\omega_c \omega_p^2}{\omega\left(\omega^2 - \omega_c^2\right)}\right), \varepsilon_3 = \varepsilon_0 \left(1 - \frac{\omega_p^2}{\omega^2}\right).$$

where the ω_p is the plasma oscillation frequency, is the cyclotron frequency and is the incident wave frequency. In the above, $\omega_p = \frac{ne^2}{m\varepsilon_0}$ and $\omega_c = \frac{eB_0}{m}$, n is plasma density (electron density), m is the electron mass, e is the magnitude of the electron charge, and is the magnetic field strength. From Maxwell's equations, the wave equation for the longitudinal electromagnetic field component in the anisotropic chiroplasma medium can be obtained as

$$\nabla_t^2 E_z + c_1 E_z + j c_2 H_z = 0 \tag{4}$$

$$\nabla_t^2 H_z + j c_3 E_z + c_4 H_z = 0 \tag{5}$$

where

$$c_1 = \frac{\left(-\beta^2 + \omega^2 \mu_0 \varepsilon_1\right)\varepsilon_3}{\varepsilon_1} + \omega\mu\gamma\left(\frac{\beta\varepsilon_2}{\varepsilon_1} + 2\omega\mu\gamma\right),$$

$$c_2 = \omega\mu\left(\frac{\beta\varepsilon_2}{\varepsilon_1} + 2\omega\mu\gamma\right),$$

$$c_3 = -\frac{\beta\omega\varepsilon_2\varepsilon_3}{\varepsilon_1} - \frac{\beta^2\gamma\varepsilon_3}{\varepsilon_1} + \frac{\beta\gamma^2\varepsilon_2\omega\mu}{\varepsilon_1} + \frac{\omega^2\mu\gamma{\varepsilon_2}^2}{\varepsilon_1} - \omega\left(\omega\mu\gamma\left(\varepsilon_1 + \varepsilon_3 + 2\mu\gamma^2\right)\right) + \beta^2\gamma,$$

$$c_4 = \frac{\omega^2\mu({\varepsilon_1}^2 - {\varepsilon_2}^2)}{\varepsilon_1} - \beta^2 + 2\omega^2\mu^2\gamma^2 - \frac{\varepsilon_2\beta\omega\mu\gamma}{\varepsilon_1}.$$

The total electric and magnetic fields in the chiroplasma medium can be expressed in the form

$$\boldsymbol{E} = \boldsymbol{E}_+ + \boldsymbol{E}_- \tag{6}$$

$$\boldsymbol{H} = j\left(\alpha_+ \boldsymbol{H}_+ + \alpha_- \boldsymbol{H}_-\right) \tag{7}$$

Moreover, the EM field can be split into longitudinal and transverse components as

$$\boldsymbol{E} = \hat{e}_z \boldsymbol{E}_z + \boldsymbol{E}_t \tag{8}$$

$$\boldsymbol{H} = \hat{e}_z H_z + \boldsymbol{H}_t \tag{9}$$

The two wave numbers in the chiroplasma medium are defined as

$$k_\pm^2 = \left(c_1 + c_4 \pm \sqrt{\left(c_1 - c_4\right)^2 - 4c_2c_3}\right)/2 \tag{10}$$

Solutions of longitudinal field components in core can be written as

$$E_{z2} = \left[A_m J_m\left(k_+\rho\right) + B_m J_m\left(c_-\rho\right)\right] \mathrm{e}^{j(\mathrm{m}\varphi - \beta z)} \tag{11}$$

$$H_{z2} = j\left[A_m\alpha_+ J_m\left(k_+\rho\right) + B_m\alpha_- J_m\left(k_-\rho\right)\right] \mathrm{e}^{j(\mathrm{m}\varphi - \beta z)} \tag{12}$$

where $\alpha_\pm = \left(c_1 - k_\pm^2\right)/c_2$, A_m and B_m are unknown coefficients. The transverse field components in the guide core can be derived to be

$$E_\rho = j/\rho\{A_m\left((u+\alpha_+ w)\rho k_{c+} J_m'\left(k_{c+}\rho\right) + (b-\alpha_+ x)m J_m\left(k_{c+}\rho\right)\right) + B_m\left((u+\alpha_- w)\rho k_{c-} J_m'\left(k_{c-}\rho\right) + (b-\alpha_- x)m J_m\left(k_{c-}\rho\right)\right)\}\mathrm{e}^{j(\mathrm{m}\varphi - \beta z)} \tag{13}$$

$$E_\varphi = -1/\rho\{A_m\left((u+j\alpha_+ x)\rho k_{c+} J_m'\left(k_{c+}\rho\right) + (u+\alpha_+ w)m J_m\left(k_{c+}\rho\right)\right) - B_m\left((v+j\alpha_- x)\rho k_{c-} J_m'\left(k_{c-}\rho\right) + (u+\alpha_- w)m J_m\left(k_{c-}\rho\right)\right)\}\mathrm{e}^{j(\mathrm{m}\varphi - \beta z)} \tag{14}$$

$$H_\rho = 1/\rho\{A_m\left((\alpha_+ u - y)\rho k_{c+} J_m'\left(k_{c+}\rho\right) + (z+\alpha_+ v)m J_m\left(k_{c+}\rho\right)\right) - B_m\left((\alpha_- u - y)\rho k_{c-} J_m'\left(k_{c-}\rho\right) + (z+\alpha_- u)m J_m\left(k_{c-}\rho\right)\right)\}\mathrm{e}^{j(\mathrm{m}\varphi - \beta z)} \tag{15}$$

$$H_\varphi = j/\rho\{A_m\left(\left(y-\alpha_+ u\right)m k_{c+} J_m\left(k_{c+}\rho\right) - (z - j\alpha_+ v)\rho J_m'\left(k_{c+}\rho\right)\right) + B_m\left(\left(y-\alpha_- u\right)m J_m\left(k_{c-}\rho\right) - (z - j\alpha_- u)\rho k_{c-} J_m'\left(k_{c-}\rho\right)\right)\}\mathrm{e}^{j(\mathrm{m}\varphi - \beta z)} \tag{16}$$

where

$$u = \frac{c_3\omega\mu\varepsilon_2 - c_4\beta\varepsilon_3}{\varepsilon_1(c_{p1}c_{p4} + c_{p2}c_{p3})},$$

$$v = -\frac{c_3\omega\mu\varepsilon_2}{c_{p1}c_{p4} + c_{p2}c_{p3}},$$

$$w = -\frac{c_1\omega\mu\varepsilon_2 + c_{p4}\beta\varepsilon_3}{\varepsilon_1(c_{p1}c_{p4} + c_{p2}c_{p3})},$$

$$x = -\frac{c_1\omega\mu}{c_1c_4 + c_2c_3},$$

$$y = -\frac{c_3\beta\varepsilon_3}{\varepsilon_1(c_1c_4 + c_2c_3)},$$

$$z = \frac{p_4\omega\varepsilon_3}{c_{p1}c_{p4} + c_{p2}c_{p3}}.$$

3. The dispersion equation

The boundary of the guide medium is defined as a DB media. The characteristic equation is obtained by using the boundary conditions at the boundaries of the chiroplasma and the DB defined medium. According to the nature of the DB boundary conditions, the normal components of electric and magnetic fields vanishes at the surface of the guide. Using the notations of this paper, they can be written as below [11-17]

$$E_\rho = 0 \text{ at } \rho = b \tag{17}$$

$$H_\rho = 0 \text{ at } \rho = b \tag{18}$$

By using the boundary conditions defined in equations (17) and (18), two equations are found, and the determinant made by the coefficients of these equations must be equal to zero to get a non-trivial solution, which yields

$$\begin{bmatrix} (u+\alpha_+ x)\rho k_+ J_m'(k_+\rho)+(v-\alpha_+ x)mJ_m(k_+\rho) & (u+\alpha_- w)\rho k_- J_m'(k_-\rho)+(v-\alpha_- x)mJ_m(k_-\rho) \\ (\alpha_+ a-e)\rho k_+ J_m'(k_+\rho)+(f+\alpha_+ b)mJ_m(k_+\rho) & -(\alpha_- a-e)\rho k_- J_m'(k_-\rho)-(f+\alpha_- b)mJ_m(k_-\rho) \end{bmatrix} \begin{bmatrix} A_m \\ B_m \end{bmatrix} = 0 \tag{19}$$

The determinant of the above matrix is set to be equal to zero to have non-trivial solutions

$$\begin{vmatrix} (u+\alpha_+ x)\rho k_+ J_m'(k_+\rho)+(v-\alpha_+ x)mJ_m(k_+\rho) & (u+\alpha_- w)\rho k_- J_m'(k_-\rho)+(v-\alpha_- x)mJ_m(k_-\rho) \\ (\alpha_+ a-e)\rho k_+ J_m'(k_+\rho)+(f+\alpha_+ b)mJ_m(k_+\rho) & -(\alpha_- a-e)\rho k_- J_m'(k_-\rho)-(f+\alpha_- b)mJ_m(k_-\rho) \end{vmatrix} = 0 \tag{20}$$

This leads to the following characteristic equation

$$f(\beta) = \begin{vmatrix} (u+\alpha_+ x)\rho k_+ J_m'(k_+\rho)+(v-\alpha_+ x)mJ_m(k_+\rho) & (u+\alpha_- w)\rho k_- J_m'(k_-\rho)+(v-\alpha_- x)mJ_m(k_-\rho) \\ (\alpha_+ a-e)\rho k_+ J_m'(k_+\rho)+(f+\alpha_+ b)mJ_m(k_+\rho) & -(\alpha_- a-e)\rho k_- J_m'(k_-\rho)-(f+\alpha_- b)mJ_m(k_-\rho) \end{vmatrix} \tag{21}$$

The above expression (21) leads to the characteristics curve that determines the propagation constants and the cutoff frequencies of the propagating modes. The energy flow can be obtained using the following relation with equations (12)-(16)

$$S_z = \frac{1}{2} Re(\boldsymbol{E} \times \boldsymbol{H}) \cdot \hat{e}_z = \frac{1}{2} Re(E_\rho H_\varphi^* - E_\varphi H_\rho^*) \tag{22}$$

4. Results and discussions

In this section, the dispersion curves and the energy flux in the cylindrical waveguide filled with an anisotropic plasma chiral medium under DB boundary conditions. It is assumed that $\mu_t = \mu_z = \mu_0$, throughout the presented computations. The longitudinal propagation constant β can be obtained numerically from the characteristics equation (20) and the relationship of the constants A_m, B_m, C_m, and D_m. To check the accuracy of the presented formulations, the result of a limited case of $\omega_p = 0$ and $\gamma = 0$ is compared with results published in [19]. The results of this paper formulation are found to approach the results in [19] very accurately.

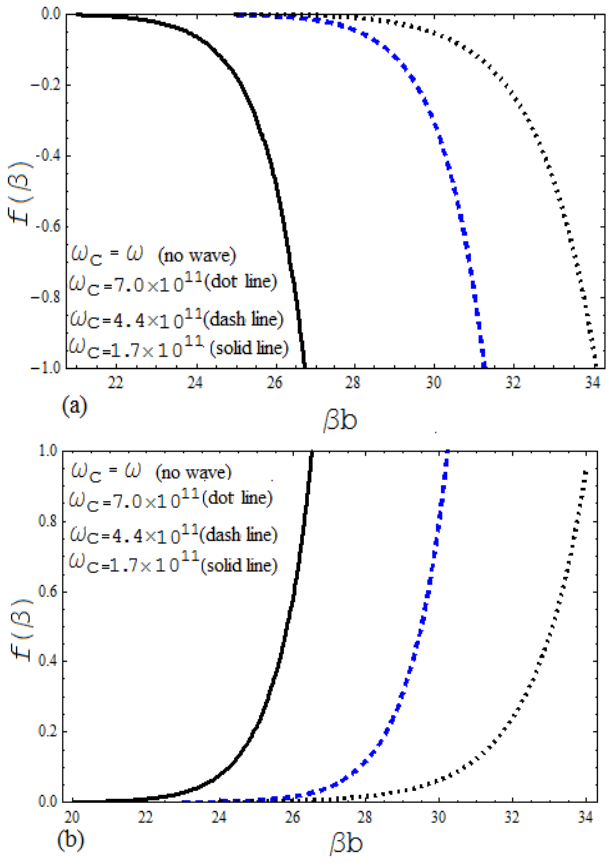

Fig.1. Characteristics curves for different values of cyclotron frequency for (a) mode H_{01} *and (b) mode* H_{11}.

Fig. (1a) and (1b) illustrate the behavior of $f(\beta)$ against βb from equation (21) for the guided mode and the guided mode for different values of the cyclotron frequencies at *b=5000* micron, $\omega_p = 6.32\times10^{11}\,Hz$, $\omega_p = 6.32\times10^{11}\,Hz$ and $\gamma = 2.0$ with $\omega_c = 7.0\times10^{11}\,Hz$ (dotted line), $\omega_c = 4.4\times10^{11}\,Hz$ (dashed line) and $\omega_c = 1.7\times10^{11}\,Hz$ (solid line). The effect of the cyclotron frequency on the characteristics curves is depicted in figure (1a) and figure (1b). It is observed from the obtained numerical results that when the cyclotron frequency is low the cut off is high and vice versa. It is also noted that curves are inverted in the case of the lowest mode, which indicates the existence of backward propagating waves. Figures 2a and 2b are the numerical results of equation (21), they demonstrate the behavior of $f(\beta)$ for βb corresponding to the modes H_{11} and H_{21}

respectively, at $\gamma = 2.0$, $\omega_p = 1\times10^{14}\,Hz$, and $\omega_c = 3.12\times10^{14}\,Hz$ at operating wavelength of 1.55 micron. As can be seen from these two Figures, the cut-off frequency of the H_{11} mode is located at values higher than that of the H_{21}. When the guide core radius is smaller; the cut-off frequency is getting higher and vice versa.

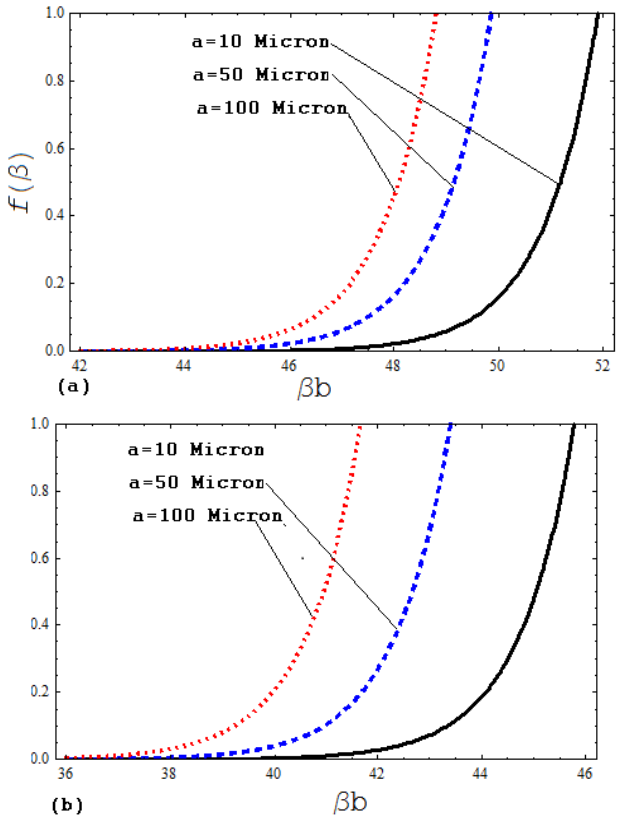

Fig.2. Characteristics curves for different cylinders' radius (a) mode H_{11} and (b) mode H_{21}.

Figs. 3(a) and 3(b) show the variation of the normalized energy flux density with respect to for the H_{01} mode for different values of the cylinder's radius and different values of the chirality. Figure 3(a) depicts the normalized energy flux density at $\omega_p = 1\times10^{14}\,Hz$, $\omega_c = 3.12\times10^{14}\,Hz$ and $\gamma = 2.0$, with *b=10* micron (solid line), *b=50* micron (dashed line), and *b=100* micron (dotted line). Figure 3(b) depicts the normalized energy flux density at *b=10* micron with $\gamma = 2.0$, $\gamma = 1.0$ and $\gamma = 0.5$ for solid line, dashed lines and dotted lines respectively. In this guided mode, the energy flux density is always oriented in the forward direction and it is higher in larger chiroplasma cylinders as expected. However, lower chirality values drive higher energy flux density in the waveguide.

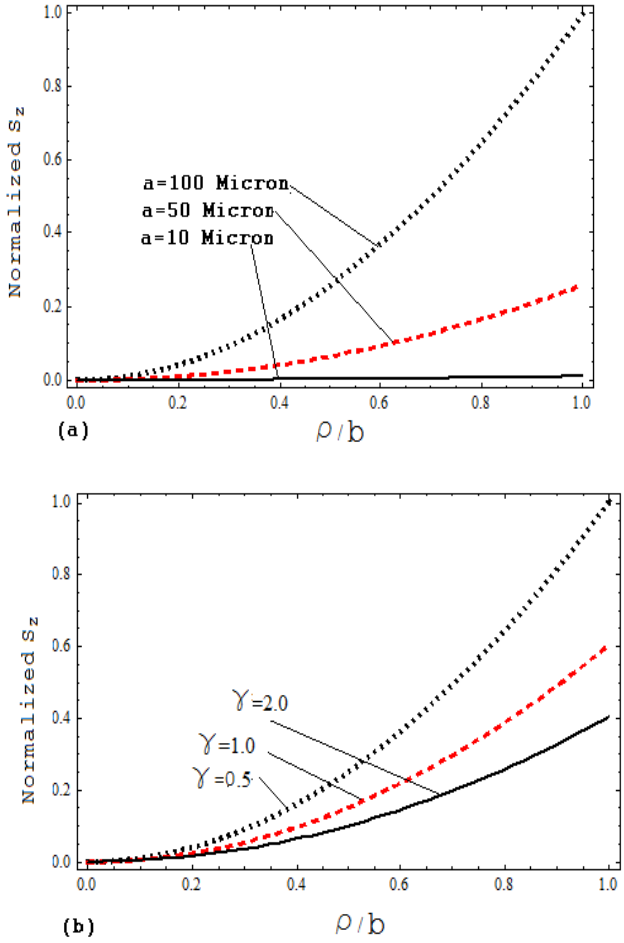

Fig.3. The energy flux density in the H_{01} mode (a) for different values of cylinders' radius (b) for different values of chirality.

Figs. 4(a) and 4(b) show the variation of the normalized energy flux density with respect to ρ / b for the H_{11} mode for different values of the cylinder's radius and different chirality parameter's values. Figure 4(a) shows variation of the normalized energy flux density at $\gamma = 2.0$, with *b=10* micron (solid line), *b=50* micron (dashed line), and *b=100* micron (dotted line). Figure 4(b) shows variation of the normalized energy flux density at $\omega_p = 1\times10^{14}\,Hz$, $\omega_c = 3.12\times10^{14}\,Hz$, and *b=10* micron with $\gamma = 2.0$, $\gamma = 1.0$ and $\gamma = 0.5$ for solid line, dashed lines and dotted lines respectively. In this guide mode, it is observed that for smaller chiroplasma filled region, the energy flux density increases in the negative direction. In this guide mode, lower chirality values have more energy flux density oriented in the negative direction. The negative flux propagation can be understood as backward wave phenomenon, which is the further evident in chiroplasma guides with lower chirality.

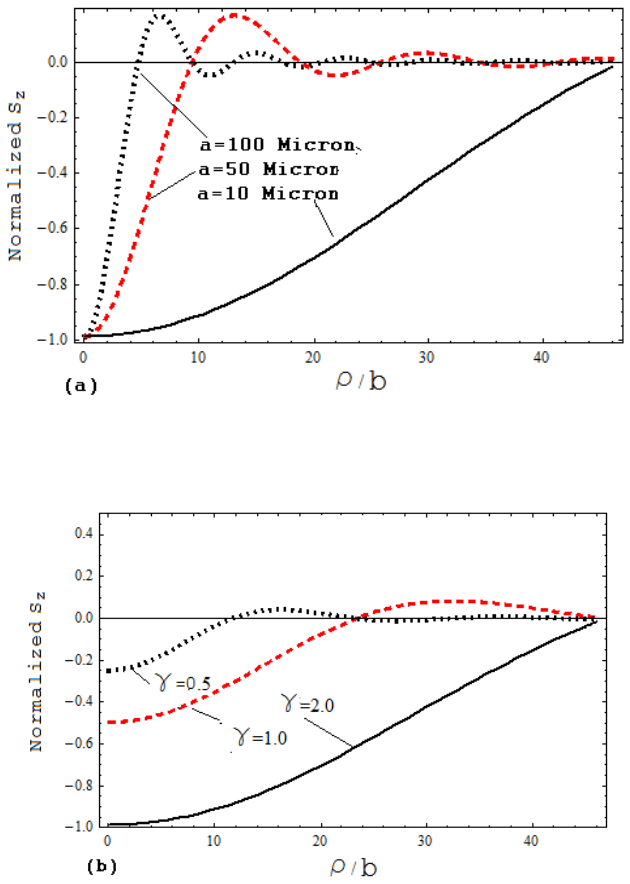

Fig.4. The energy flux density in the H_{11} mode (a) for different values of cylinders' radius (b) for different values of chirality.

Figs. 5(a) and 5(b) show the variation of the normalized energy flux density with respect to for the mode for different values of the cylinder's radius and different chirality parameter's values. Figure 5(a) shows variation of the normalized energy flux density at $\omega_p = 1\times10^{14}\,Hz$, and $\omega_c = 3.12\times10^{14}\,Hz$ $\gamma = 2.0$, with *b=10* micron (solid line), *b=50* micron (dashed line), and *b=100* micron (dotted line). Figure 5(b) shows the variation of the normalized energy flux density at *b=10* micron with $\gamma = 2.0$, $\gamma = 1.0$ and $\gamma = 0.5$ for solid line, dashed lines and dotted lines respectively. In this guided mode, it is observed that the small chiroplasma filled region is embossed by negative values of the energy flux density and when the chiroplasma region is extended, the energy flux tends to increase to positive values. Similarly lower chirality values instigate negative energy flux densities and higher chirality values instigate positive energy flux densities.

The effect of the plasma frequency on the propagation of electromagnetic waves in plasma chirowaveguide is investigated in Figures 6(a) and 6(b). These figures illustrate the variation the energy flux densities with respect to ρ / b for the H_{01} and H_{11} modes at $\omega_c = 3.12\times10^{14}\,Hz$, $\gamma = 2.0$ Figure 6(a) shows variation the energy flux densities with respect to ρ / b for different values of plasma frequency in the guide for the H_{01} mode. It is shown that if the plasma frequency is increased then the magnitude of the energy flux density increased and all of the energy in the guide is positive. Figure 6(b) shows variation the energy flux densities with respect to ρ / b for different values of plasma frequency for the H_{11} mode. To the contrary of the H_{01} mode, it is shown that for the H_{11} mode, the increase in the plasma frequency yields, mostly, an increase of the energy flux density in the negative orientation. This is a noteworthy phenomenon.

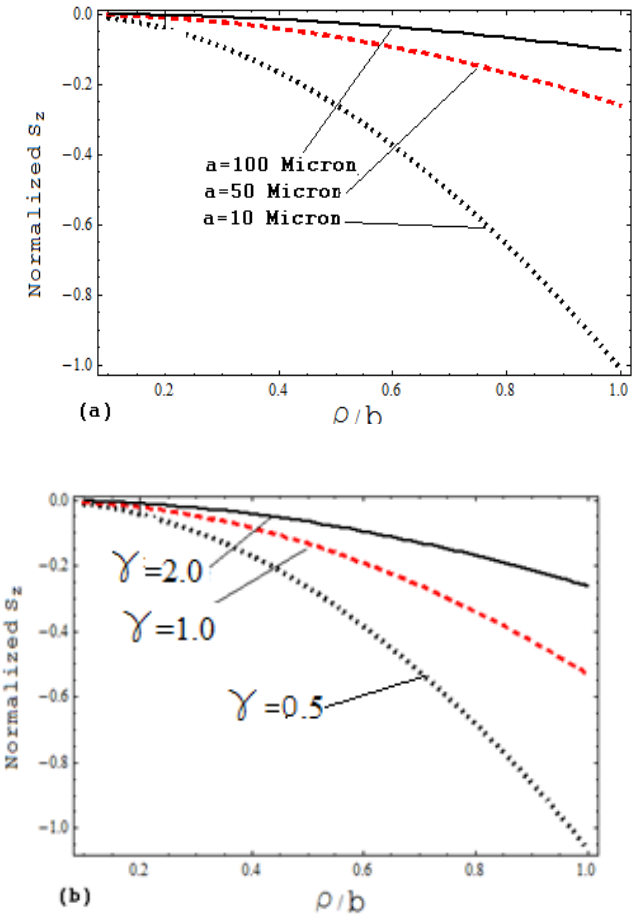

Fig.5. The energy flux density in the H_{21} mode for (a) different values of cylinders'radius (b) different values of chirality.

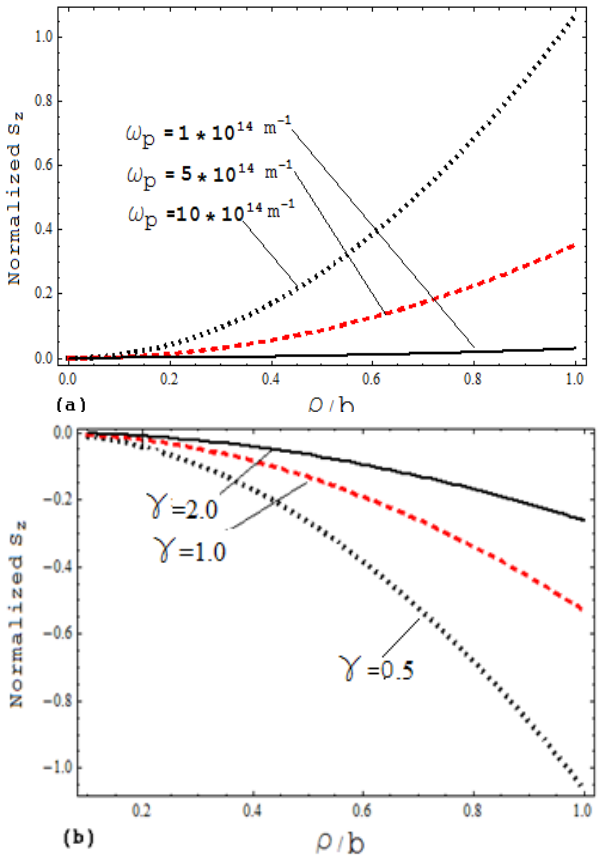

Fig.6.The energy flux density for different values of plasma frequency (a) mode H_{01} *and (b) mode* H_{11}.

5. Conclusions

The wave propagation in a circular anisotropic chiroplasma waveguide with the outer surface coated with a DB boundary has been studied and analyzed in this paper. The dispersion diagram, cut-off frequencies and the propagating modes in the chiroplasma-filled circular waveguide have been numerically examined. The effect of the chirality parameter of the guide medium, the guide dimensions, and the plasma frequency on the propagation of the energy flux density is studied thoroughly. It is noted that maximum of the flux density concentrated in the core of the waveguide. Furthermore, it has been found that both forward and backward waves are supported by the waveguide material structure. The negatively oriented energy flux is exited in higher modes in the circular chiroplasma waveguide and its intensity is controlled by the guide size, the chirality parameter, and the plasma frequency of the guide material. At certain values of plasma frequency, the energy flux may invert its orientation from negative to positive values. These characteristics might give this waveguide a great potential for advanced applications as in the development of novel EM tools.

Acknowledgement

The authors would like to extend their sincere appreciation to the Deanship of Scientific Research (DSR) at King Saud University for its funding of this research through the Research Group Project no RG-1436-001.

References

[1] P. Pelet, N. Engheta, Antennas and Propagation, IEEE Transactions on, **38**, 90 (1990).
[2] A. L. Topa, C. R. Paiva, and A. M. Barbosa, Microwave Theory and Techniques, IEEE Transactions on, **42**, 629 (1994).
[3] I. V. Lindell, A. Sihvola, S. Tretyakov, A. Viitanen, "Electromagnetic waves in chiral and bi-isotropic media," 1994.
[4] S. Gulistan, A. Syed, Q. Naqvi, Journal of Electromagnetic Waves and Applications **26**, 2130 (2012).
[5] M. M. Ali, M. J. Mughal, A. A. Rahim, Q. A. Naqvi, International Journal of Applied Electromagnetics and Mechanics, **38**, 139 (2012).
[6] S. Viitanen, Progress In Electromagnetics Research, **39**, 265 (2003).
[7] J.-F. Dong, J. Li, Progress In Electromagnetics Research, **124**, 331 (2012).
[8] J.-F. Dong, J. Li, International Journal of Applied Electromagnetics and Mechanics, **40**, 283 (2012).
[9] M. Baqir, P. Choudhury, Journal of Electromagnetic Waves and Applications, **26**, 2165 (2012).
[10] A. Ghaffar, M. A. Alkanhal, Optical Materials Express, **4**, 1756 (2014).
[11] B. Hu, C. Ruan, Journal of Physics D: Applied Physics, **31**, 2151 (1998).
[12] J. Gong, Journal of plasma physics, **62**, 87 (1999).
[13] J. Gong and S. Yang, in Microwave Conference Proceedings, 1997. APMC'97, 1997 Asia-Pacific, 1997, pp. 793-796.
[14] I. V. Lindell, A. Sihvola, Physical Review E, **79**, 026604 (2009).
[15] I. V. Lindell and A. H. Sihvola, Progress In Electromagnetics Research Letters, **6**, 131 (2009).
[16] I. V. Lindell and A. Sihvola, Microwave Theory and Techniques, IEEE Transactions on, **58**, 903 (2010).
[17] M. Baqir and P. Choudhury, Journal of Nanomaterials, **2014**, 2 (2014).
[18] M. Baqir and P. Choudhury, Optik-International Journal for Light and Electron Optics, **125**, 2950 (2014).
[19] M. Baqir and P. Choudhury, Journal of Electromagnetic Waves and Applications, **27**, 783 (2013).

*Corresponding author: aghaffar16@uaf.edu.pk; majeed@ksu.edu.sa